

Dynamical coupling between locomotion and respiration

Andreas Daffertshofer, Raoul Huys, Peter J. Beek

Faculty of Human Movement Sciences, Institute for Fundamental and Clinical Human Movement Sciences, Vrije Universiteit, Van der Boechorststraat 9, 1081 BT Amsterdam, The Netherlands

Received: 4 June 2003 / Accepted: 23 December 2003 / Published online: 3 March 2004

Abstract. In search of the formative principles underlying locomotor-respiratory coupling, we reanalyzed and modeled the data collected by Siegmund and coworkers (1999) on the synchronization of respiration during rowing. Apart from the frequency doubling in respiration reported earlier, detailed time-resolved spectral analyses revealed decreasing stability of entrainment close to abrupt changes in frequency relations as well as switches in the relative phase between respiration and locomotion. A single physiological, albeit mechanically constrained, quantity sufficed to explain the observed frequency and phase locking phenomena: the effective value of oxygen volume in the lungs. The cyclic abdominal pressure modulates the self-sustaining rhythmic respiration, modifies the total lung pressure, and causes (local) maxima at frequency ratios between movement and respiration that are composed of small integers. Hence, optimizing the effective oxygen volume can be seen as the mechanism that drives respiration to synchronize with locomotion.

1 Introduction

Moving about requires task-specific coordination of both homogeneous and heterogeneous subsystems. This becomes particularly apparent during sustained, rhythmic activities. As a case in point, respiration is often coupled to locomotion in animals and humans alike. For instance, in various quadrupeds, locomotor-respiratory coupling (LRC) is evident in the prevalence of 1:1 and 2:1 frequency ratios between the cyclic leg movements and rhythmic breathing (e.g., Young et al. 1992; Hoppensteadt 1997; Boggs 2002; Bramble and Jenkins 1993). In humans, LRC has been studied, for example, during cycling (Kohl et al. 1981; Bernasconi and Kohl 1993), running (Bramble and Carrier 1983; Bernasconi et al. 1995), wheelchair propulsion (Amazeen et al.

2001), and rowing (Mahler et al. 1991a,b; Siegmund et al. 1999). Besides a variety of different frequency relations, including 1:1, 2:1, 3:1, 3:2, and 5:2, humans regularly show transitions between different locking modes (Bramble and Carrier 1983). Despite the abundance of such empirical findings, however, the mechanisms underlying LRC are far from understood. Indeed, over the years several explanations for LRC have been put forward, but none of these has yet been able to account for the broad range of empirical phenomena encountered while explicitly addressing the constraints acting upon the participating subsystems.

As an important step in understanding the cyclic nature of respiration, Del Negro and coworkers (2002a,b) recently showed how a dedicated neural network might generate a breathing rhythm in mammals. In brief, irrespective of whether or not pacemaker neurons are present, the structure of the respiratory network readily induces oscillatory behavior. Therefore, respiration can be seen as (a product of) a self-sustaining oscillator. In this context, recall that every biological system can be described formally in terms of its dynamics. Such a description is only feasible when concentrating on the most relevant features. In general, candidate features are self-organized structures in the form of coherent macroscopic patterns that arise from interacting subsystems. Their dynamics and, in particular, their stability properties can be rigorously formalized by mathematical concepts of pattern formation. To apply these concepts to biological movements, we focus on coordinative structures as this term readily implies that microscopic components (neurons, muscle fibers, etc.) interact with each other to generate a few macroscopic quantities that reflect ordered states of the system. Being constrained to act as functional units, such coordinative neuromuscular assemblies and their stability can be addressed via emergence, disappearance, or transitions between ordered states. Transitions are of pivotal importance in this regard because in their immediate vicinity, i.e., close to changes in coordination, one can confine oneself to the (low-dimensional) dynamics reflecting the changing order imposed on the

entire set of subcomponents in a self-organized manner (Haken 1996, 2000). Coming back to the issue of LRC, more specific coordination modes are cyclic movements that are commonly viewed as (a result of) self-sustaining oscillators or stable limit cycles (e.g., Keith and Rand 1984; Kay et al. 1987; Kelso 1995; Beek et al. 1996; Haken 1996; Glass 2001). With locomotion as voluntary cyclic movement and respiration we have two self-sustaining oscillations at hand and it becomes prudent to ask what mechanisms are implicated in their synchronization. Adopting a dynamical systems perspective, we address this question by looking for necessary features in the dynamic interaction between locomotion and respiration. We formulate a dynamical model that accounts for LRC by means of frequency and phase locking and transitions between locking states involving loss of stability of a given mode-locked state and the simultaneous stabilization of another. Following a more qualitative description of the oscillatory processes, we concentrate on the explicit nature of the coupling, which turns out to be the effective value of oxygen volume in the lungs, that is, a single physiological, albeit mechanically constrained, measure.

The present work was inspired by recent findings concerning LRC in rowing. Siegmund and coworkers (1999) investigated LRC in experienced oarsmen when performing a simulated 2-km race on a rowing ergometer. Besides various ventilation parameters, such as respiration frequency, tidal volume, and the volumes and pressures of oxygen uptake and expired carbon dioxide, the ergometer handle force was recorded. LRC was assessed in terms of the ratio between the averages over consecutive 10-s intervals of instantaneous ventilation rate vs. instantaneous stroke rate. As is illustrated in Fig. 1a, b, and c, stable entrainment patterns of 1:1, 1:2, and 1:3 were observed between the rowing strokes and respiration.

In addition to stable LRC entrainment, however, some rowers also showed switches in frequency locking. First of all, transitions from a 1:1 locking to a 1:2 locking occurred, which appeared to be preceded by an increasing peak-width around the dominant frequency, hinting at a loss of stability of the 1:1 locking. Furthermore, switches of about 90° occurred in the relative phase (which was defined as $\Delta\phi = P\varphi_{\text{stroke}} - Q\varphi_{\text{resp}}$ in the case of a $Q:P$ frequency locking between stroke rate and respiration).

Given the presence and characteristics of qualitative changes in entrainment in terms of switches in frequency or phase locking, the underlying mechanism should, in general, allow for phase transitions, that is, spontaneous changes in the organization among the contributing subsystems or components (see, e.g., Nicolis and Prigogine 1989; Haken 2000). The central focus of the present study is therefore the (qualitative) form of the coupling or interaction between these

components, which, of course, have to be identified first. In view of the physically demanding rowing performance,¹ one might think of the energy exchange through the lungs when looking for possible entrainment causes. Along these lines we assume that the time-dependent oxygen volume in the lungs is modulated by the inhalation/exhalation cycle and the movement-related lung pressure.

2 LRC dynamics – entrainment

To model LRC we start off with two distinct processes: respiration and movement. While respiration can be quantified directly via the inhaled/exhaled air, we first consider which aspects of the rowing movements may affect lung pressure and, thus, the respiration dynamics. During each rowing stroke various forces act via the rib cage on the lungs. At the beginning of the drive, i.e., when the legs are flexed and the arms and torso are extended, the visceral mass compresses the abdominally apposed lung volume. The compression vanishes as soon as the legs extend, but it returns when the abdominal muscles become maximally active at the final part of the drive. During mid-recovery, this muscle-activity-induced compression again disappears. Thus, during a single rowing stroke the lung volume is compressed twice (Rodriguez et al. 1990; Wasjweller et al. 2000). Notice that this (double) frequency is readily apparent from the fact that the intra-abdominal pressure during a single stroke contains two peaks (Manning et al. 2000). Hence the frequency locks between handle forces and breathing rhythms observed by Siegmund and colleagues do not reflect the frequency locking between movement lung pressure oscillations and respiration: when mapping from handle force to lung pressure dynamics, the aforementioned locking ratios, 1:1, 1:2, or 1:3, should be understood as 2:1, 1:1, or 2:3, respectively.

Mathematically, we quantify the inhalation/exhalation cycle, or the respiration for short, by the time-dependent variable $R(t)$ and the movement-related lung pressure by $M(t)$. Independence of these two quantities implies a productive (multiplicative) impact on the resulting oxygen volume in the lungs, here denoted by $VO_2(t)$.² This assumption can be formalized as

$$VO_2(t) = [R_0 - R(t)][M_0 - M(t)] , \quad (1)$$

where R_0 and M_0 denote finite amplitudes or offsets around which the dynamical components $R(t)$ and $M(t)$ oscillate. Although this time-dependent oxygen volume represents a measure of energy exchange, its oscillatory nature implies that the relevant (physical) quantity is its

¹Notice that the simulated race represented a maximal test. The maximum respiratory exchange ratio exceeded 1.15 in nearly all participants, and peak heart rate exceeded its predicted maximum (220 – age).

²The quantity $M(t)$ should not be confused with the stroke movement. Whenever necessary, we distinguish between lung pressure dynamics and stroke dynamics by indices “ M ” or “stroke”.

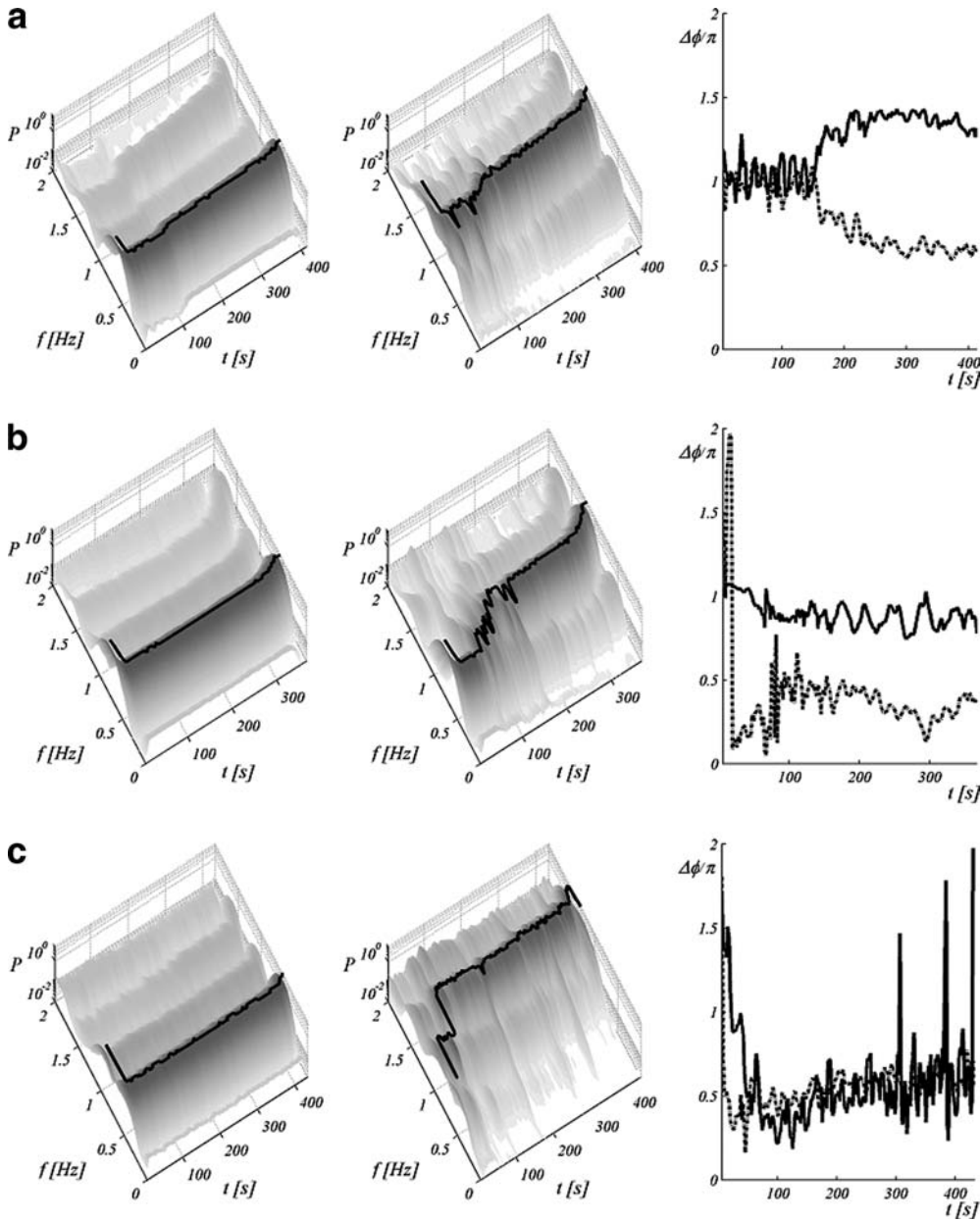


Fig. 1a. Using the data from Siegmund et al. (1999), we computed spectrograms for both force data (*left panel*) and respiration (*middle panel*): over consecutive finite time windows (length 10 s or roughly five periods of the movement frequency) the power spectral density was estimated using Welch's periodogram method (see Matlab 6.5, Mathworks, Natick, MA). The relation between the frequencies with the maximal spectral power, ω_{stroke} and ω_{resp} , reflects the ratio of frequency locking, here consistently $\omega_{\text{stroke}} : \omega_{\text{resp}} = 1 : 2$, while the width of the spectral peak indicates the locking strength. In addition to the spectral distribution, we computed the Fourier strength at the dominant frequency per window for each of the signals. These phases were subtracted from each other so as to obtain the relative Fourier phase between respiration and force; *right panel*: *solid line*

$\Delta\phi = \varphi_{\text{stroke}}(\omega_{\text{stroke}}) - \varphi_{\text{resp}}(\omega_{\text{stroke}})$ and *dashed line* $\Delta\phi = 2\varphi_{\text{stroke}}(\omega_{\text{stroke}}) - \varphi_{\text{resp}}(2\omega_{\text{stroke}})$. While frequency remains stably locked at 1:2, the respective relative phases switch by approximately 90°

Fig. 1b. See Fig. 1a for further details. This subject shows a transition in frequency locking from $\omega_{\text{stroke}} : \omega_{\text{resp}} = 1:1$ to $\omega_{\text{stroke}} : \omega_{\text{resp}} = 1:2$, while the relative phase remains essentially unaltered

Fig. 1c. See Fig. 1a for further details. After an initial switch this subject shows a consistent frequency locking at $\omega_{\text{stroke}} : \omega_{\text{resp}} = 1:3$ with an essentially constant relative phase; note that in contrast to Fig. 1a and b the relative phase reads $\Delta\phi = \varphi_{\text{stroke}}(\omega_{\text{stroke}}) - \varphi_{\text{resp}}(\omega_{\text{stroke}})$ (*solid line*) and $\Delta\phi = 3\varphi_{\text{stroke}}(\omega_{\text{stroke}}) - \varphi_{\text{resp}}(\omega_{\text{stroke}})$ (*dashed line*). See text for further explanations

effective value. Conventionally, we define the effective value of $\dot{V}O_2(t)$ over a finite time span T as

$$E(T) = \sqrt{\frac{1}{T} \int_0^T \{\dot{V}O_2(t)\}^2 dt} . \quad (2)$$

As we will demonstrate in the following, the effective value is of central importance for the specific forms of LRC in that it readily prescribes optimal ratios of frequency and phase locking between cyclic movements and breathing rhythms.

2.1 Algebraic aspects

Before entering a detailed discussion of self-sustaining dynamics, we briefly illustrate the immediate consequences of the multiplicative structure of $VO_2(t)$. For the sake of simplicity, we assume that the underlying oscillations are fully harmonic, that is, we consider

$$\begin{aligned} R(t) &= A_R \sin(\omega_R t + \varphi_R) \quad \text{and} \\ M(t) &= A_M \sin(\omega_M t + \varphi_M) \quad , \end{aligned} \quad (3)$$

where ω_R is the respiration frequency, ω_M denotes the movement/pressure frequency, and φ_R and φ_M represent optional phase shifts. Inserting these forms into (1), the $VO_2(t)$ reads

$$\begin{aligned} VO_2(t) &= R_0 M_0 \left[1 - \frac{A_R}{R_0} \sin(\omega_R t + \varphi_R) \right] \\ &\quad \times \left[1 - \frac{A_M}{M_0} \sin(\omega_M t + \varphi_M) \right] \quad . \end{aligned} \quad (4)$$

Without loss of generality, we rescale $VO_2(t)$ by means of $R_0 = M_0 = 1$ and fix the movement phase to $\varphi_M = 0$, yielding

$$\begin{aligned} VO_2(t) &= [1 - A_R \sin(\omega_R t + \varphi_R)] \\ &\quad \times [1 - A_M \sin(\omega_M t)] \quad . \end{aligned} \quad (5)$$

Consequently, the effective value (2), rephrased via $T = 2\pi/\omega$, i.e., $E(T) \rightarrow E(\omega)$, becomes

$$\begin{aligned} E(\omega) &= \sqrt{\frac{\omega}{2\pi} \int_0^{2\pi/\omega} \{ [1 - A_R \sin(\omega_R t + \varphi_R)] [1 - A_M \sin(\omega_M t)] \}^2 dt} \quad . \end{aligned} \quad (6)$$

This effective value represents the mean oxygen exchange in the lungs where breathing frequency is given by ω_R and the movement-related lung pressure oscillates with frequency ω_M . To illustrate the depen-

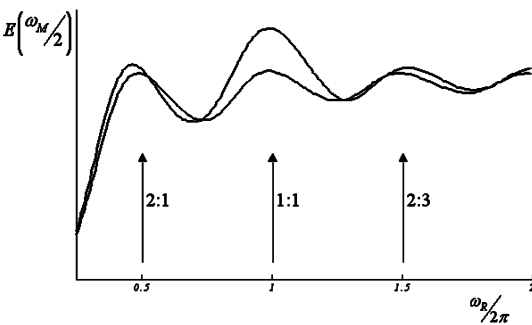


Fig. 2. $E(\omega_M/2)$ as function of ω_R ; we chose the following parameters: $\varphi_R = 0$, $A_R = 0.5$, and $\omega_M = 1$; all the frequencies are multiples of 2π . As can be seen, E has maxima at integer relations between ω_M and ω_R . Depending on the movement amplitude, however, the global maximum is either at 2:1 ($A_M = 0.2$, lower trace) or 1:1 ($A_M = 0.01$, upper trace)

dency of $E(\omega)$ on ω_R and ω_M , we utilize (6) and calculate the effective value per stroke cycle, that is, for the time span $T_{\text{stroke}} = 2T_M = 4\pi/\omega_M$. As shown in Fig. 2, the effective value of oxygen volume has (local) maxima at frequency ratios $\omega_M:\omega_R = 2:1, 1:1, 2:3$, and so on.

Recall that in the present analyses movement frequency is related to lung pressure, which oscillates twice as fast as the handle force (locomotion) as described by Siegmund et al. (1999); consequently, the ratios in Fig. 2 can be translated into $\omega_{\text{stroke}}:\omega_R = 1:1, 1:2, 1:3$, and so on. Interestingly, depending on the amplitude of one oscillator (here the movement/lung pressure amplitude A_M), the effective value becomes maximal at either $\omega_M:\omega_R = 2:1$ or $\omega_M:\omega_R = 1:1$ (for A_M small or A_M large, respectively), that is, at the most prominent frequency relations reported in Siegmund et al. (1999).

Of course, such amplitude differences might always exist when studying different subjects or tasks. However, amplitude differences are less obvious when considering a single subject in a single experimental trial. In particular, when considering spontaneous switches in LRC, i.e., different frequency locks, one should ask what might cause a possible change in amplitude. Anticipating the subsequent modeling in terms of nonlinear oscillators, we here assume that both amplitudes depend on their respective frequencies, that is, $A_R = A_R(\omega_R)$ and $A_M = A_M(\omega_M)$. The faster the movement, the smaller the amplitudes, that is, both amplitudes are assumed to drop when their respective frequencies increase, for instance, by means of the following exponential forms:

$$\begin{aligned} A_R &= A_R^{(0)} e^{-\beta_R \omega_R} \quad \text{and} \\ A_M &= A_M^{(0)} e^{-\beta_M \omega_M} \quad \text{with} \quad |A_R^{(0)}|, |A_M^{(0)}| < 1 \quad . \end{aligned} \quad (7)$$

Besides these frequency dependencies one may also think of an increasing oxygen demand in the course of a trial; note that (experienced) rowers like the ones studied by Siegmund et al. have a fairly steady rowing frequency. A fatigue-related increase in energy demand might be introduced here in the form of an exponential decay in both respiration and movement amplitudes. That decay, however, may evolve on rather different time scales, which we formulate as

$$\begin{aligned} A_R^{(0)} &= A_R^{(0)}(\tau) = A_R^{(1)} - A_R^{(2)} [1 - e^{-\gamma_R \tau}] \quad \text{and} \\ A_M^{(0)} &= A_M^{(0)}(\tau) = A_M^{(1)} - A_M^{(2)} [1 - e^{-\gamma_M \tau}] \quad . \end{aligned} \quad (8)$$

Notice that we use here τ instead of t as time variable to indicate that the time scale of the change in energy demand differs from that of both respiration and movement. We distinguish between the optimal frequency ratios at either 2:1 or 1:1 (1:1 or 1:2 in Siegmund et al.'s notation) by relating the effective values $E(\omega_M/2)$ at the corresponding respiration frequencies to each other. Put differently, we compute $E(\omega_M/2)$ at the first two harmonics relative to the one at the movement frequency:

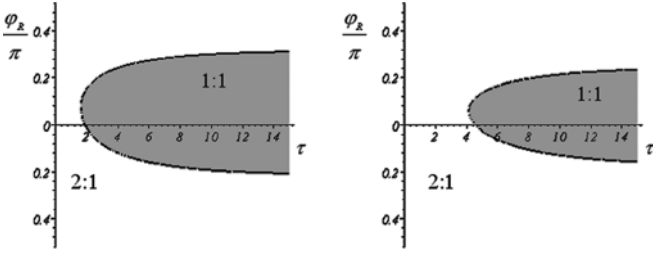


Fig. 3. Stability regimes (Arnold tongues) by means of the relation (9) depending on the (relative) phase φ_R and the “decay time” τ . For the frequency-related drop in amplitude we chose for both processes $\beta_M = \beta_R = 0.1$. The fatigue-related amplitude decrease or increase is defined via $\gamma_M = 0.2, \gamma_R = 0.0$ (*left panel*) or via $\gamma_M = 0.0, \gamma_R = 0.2$ (*right panel*), that is, either movement (*left*) or respiration (*right*) is affected; $A_M^{(1)} = 0.01, A_M^{(2)} = -0.01$ and $A_R^{(1)} = 0.5, A_R^{(2)} = 0$ (i.e., an increasing movement amplitude in the *left panel*) and $A_M^{(1)} = 0.01, A_M^{(2)} = 0$ and $A_R^{(1)} = 0.5, A_R^{(2)} = 0.2$ (i.e., a decreasing respiration amplitude in the *right panel*). In the beginning (τ small) a 2:1 frequency locking dominates. Given the presence of a proper phase relation, a lasting demand may cause a switch to 1:1 frequency locking because the effective value $E(\omega_M/2)$ might become optimal; cf. Fig. 2 for the remaining parameter and see text for further explanations

$$\Delta_M = \frac{\lim_{\omega_R \rightarrow \omega_M} E(1/2\omega_M)}{\lim_{\omega_R \rightarrow 1/2\omega_M} E(1/2\omega_M)} \dots \rightarrow \dots$$

$$\begin{cases} \geq 1 & \text{corresponds to 1:1 locking} \\ < 1 & \text{corresponds to 2:1 locking} \end{cases} \quad (9)$$

Given the amplitude changes introduced in (7) and (8), this relation turns out to cover two (or more) distinct regimes, each of which represents a certain optimal ratio of frequency locking (Fig. 3).

Thus the productive contribution of movement-related lung pressure and respiration to the oxygen volume in the lungs induces frequency relations that are locally optimal at specific ratios. Amplitude and phase relations between the two contributing oscillatory components may affect the globally optimal entrainment pattern differentially.

2.2 Dynamics

Continuing our search for mechanisms that may generate frequency-locked states, we now turn our attention to the (qualitative) dynamical properties of the underlying oscillatory subsystems and their explicit coupling. As already mentioned in the introduction, rhythmic respiration can be seen as the result of a self-sustaining oscillator (network). Similarly, the locomotion-related oscillations should be seen as the result of self-sustaining oscillations, not in the least because we consider LRC in the context of voluntary rhythmic movements. In order to concentrate on the essential features of entrainment patterns, we here abstain from formulating the corresponding oscillators in physiological terms but rather consider generic forms of stable limit cycles. Formally, their dynamics may be cast into

$$\begin{aligned} \ddot{R} + \omega_R^2 R + n_R(R, \dot{R}) &= J_{R \leftarrow M} \text{ and} \\ \ddot{M} + \omega_M^2 M + n_M(M, \dot{M}) &= J_{R \rightarrow M} \end{aligned} \quad (10)$$

$R = R(t)$ represents the respiratory component with eigenfrequency ω_R , $M = M(t)$ is the movement-related oscillator (eigenfrequency ω_M), and n_R and n_M are nonlinear functions stabilizing the oscillators’ amplitudes; see below for their specific forms. The dot notation refers to temporal derivatives.

Most important in this dynamical structure is that the two oscillators in (10) are mutually coupled: via the function $J_{R \leftarrow M}$ movement affects respiration, and via $J_{R \rightarrow M}$ the latter is fed back into the movement dynamics. To specify these coupling functions, we take up the results of the previous section and assume that respiration adapts to movement so as to obtain an optimal effective value of oxygen volume in the lungs. Put differently, we formally introduce a constraint by means of maximization of the effective value of $VO_2(t)$ as defined in (2). For the sake of legibility, however, we use E in its squared form so that its maximization coincides with a vanishing variation of E^2 . Recall that in all the aforementioned experimental trials movement frequency remained fairly constant. Hence, we restrict the discussion to the case in which respiration is adjusted, but movement barely. In other words, we concentrate on the variation of E^2 with respect to $R(t)$ that has to vanish whenever a solution gives rise to an optimal energy transfer. That is, we use

$$E^2 = \frac{1}{T} \int_0^T \{VO_2(t)\}^2 dt \stackrel{!}{=} \max \Rightarrow \frac{\delta E^2}{\delta R(t)} \stackrel{!}{=} 0,$$

which, when substituting the effective value (2), becomes

$$\frac{\delta E^2}{\delta R(t)} = [R(t) - R_0][M(t) - M_0]^2 = 0. \quad (11)$$

Indeed, this form will serve as coupling function between respiration and locomotion. In view of the nearly constant movement frequency we ignore the coupling from respiration to movement, i.e., $J_{R \rightarrow M} = 0$ – to the best of our knowledge voluntarily chosen breathing rhythms have only weak, if any, effects on locomotion. When scaling the overall coupling strength by a fixed parameter α , our model finally reads³

$$\ddot{R} + \omega_R^2 R + n_R(R, \dot{R}) = \alpha[R - R_0][M - M_0]^2. \quad (12)$$

As mentioned above, we refrain from defining the oscillators in physiological terms but concentrate on qualitative aspects of entrainment. Along these lines we assume that the nonlinearity n_R in (12) only consists of

³Notice that several terms in the coupling function primarily affect the intrinsic properties of the oscillator R rather than the “coupling” M with R . For instance, $\alpha R_0 M_0^2$ shifts the origin of the limit cycle and $\alpha R M_0^2$ changes the eigenfrequency ω_R .

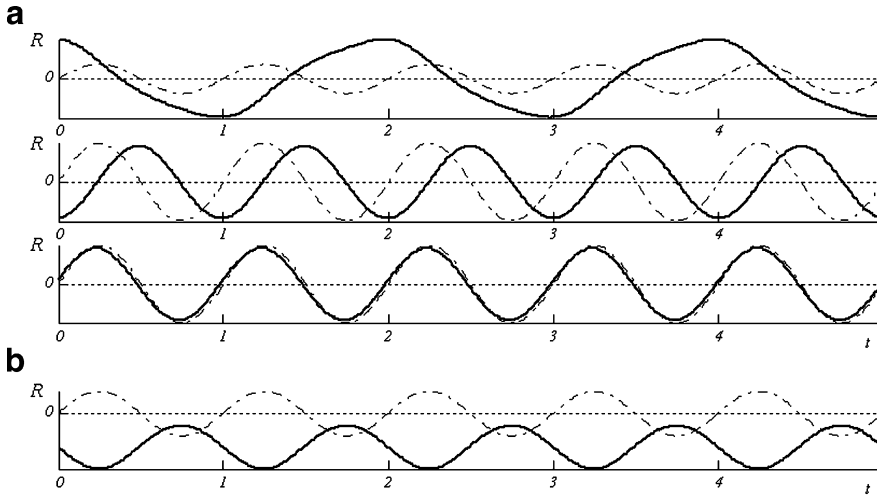


Fig. 4a. Simulation of the dynamics (14). All panels show the evolution of the respiration function $R(t)$; parameter values are $\varepsilon = 1$, $v = 1$, $\alpha = 1$, and the forcing function is $M(t) = A_M(t) \sin(\omega_M t)$, with $\omega_M = 2\pi$ dashed line in each figure; see also footnote 4. Except for the lower panel, for which we chose $A_M = 0.2$, the movement amplitude is equal to $A_M = 1$. Respiration offset is always $R_0 = 0$ (cf. Fig. 4b). In the upper panel, the movement

offset is finite $M_0 = 2.5$, leading to a 2:1 frequency locking (1:1 stroke rate/respiration entrainment). Decreasing that offset to $M_0 = 0$ causes a frequency doubling bifurcation (1:1 frequency locking in the middle panel; 1:2 stroke rate/respiration entrainment), which is followed by a change in the phase relation between $M(t)$ and $R(t)$ by 90° when movement amplitude decreases from $A_M = 1$ to $A_M = 0.2$.

low-order polynomials in R and \dot{R} . More specifically, we use a Rayleigh oscillator, which is commonly used in the study of motor control to stabilize the peak velocity of cyclic movements (e.g., Kay et al. 1987). Applied to the present problem, the Rayleigh oscillator reads

$$n_R(R, \dot{R}) = \varepsilon_R(\dot{R}^2 - v_R^2)\dot{R}. \quad (13)$$

In the absence of any forcing (i.e., for $\alpha = 0$), this oscillator is known to produce stable amplitudes that decrease monotonically with increasing frequency. Substituting (13) into (12) gives the final form of the respiration dynamics under impact of movement oscillations as

$$\ddot{R} + \omega_R^2 R + \varepsilon_R(\dot{R}^2 - v_R^2)\dot{R} = \alpha[R - R_0][M - M_0]^2. \quad (14)$$

The derived dynamics represents a self-sustaining non-linear oscillator (left-hand side) that is driven by an external force $M = M(t)$. Although this is a single force, it affects the R -system differentially – the two factors M and M^2 force the system “normally” as well as parametrically. Consequently, depending on the relation between “normal” and parametric forcing and depending on the strength of M vs. M^2 , the entrainment between R and M may differ.

As illustrated in Fig. 4, possible response patterns may include 1:1 frequency synchronization with distinct phase relations (e.g., $|\varphi_R - \varphi_M| = 0^\circ$ and 90°) or, alternatively, subharmonic responses, that is, a frequency relation of $\omega_M : \omega_R = 2 : 1$.

Patently, transitions between the different solutions might be induced by various factors. Briefly, when starting off with finite movement amplitudes and offsets one can observe a 2:1 frequency locking (upper panel

in Fig. 4a).⁴ Decreasing movement offset results in a frequency-doubling bifurcation ($\omega_M : \omega_R = 2 : 1 \rightarrow \omega_M : \omega_R = 1 : 1$; middle panel in Fig. 4a). Furthermore, reducing movement amplitude leads to a transition of the relative phase between the two oscillators while the frequencies remain 1:1 entrained (lower panel in Fig. 4a). Next to changes in the movement oscillator, a frequency-doubling bifurcation might also be realized when the offset of the respiration oscillator is increased even in the case of a finite movement offset (Fig. 4b); see, e.g., Guckenheimer and Holmes (1983) or Nayfeh and Mook (1979) for more detailed discussions on (parametrically) forced Rayleigh oscillators and corresponding bifurcation routes, especially when using the overall coupling strength (α) or the relation between the two (eigen-)frequencies as bifurcation parameters.

⁴As discussed, $M(t)$ is a self-sustaining, stable limit cycle. Thus we can cast the movement dynamics in a form similar to that of the respiration, for instance,

$$\ddot{M} + \omega_M^2 M + n_M(M, \dot{M}) = 0$$

with

$$n_M(M, \dot{M}) = \varepsilon_M(\dot{M}^2 - v_M^2)\dot{M}.$$

Since this form represents an autonomous oscillator, its solution by means of a first-order approximation (averaged solution) becomes

$$M(t) \approx A_M(\omega_M) \sin(\omega_M t) \text{ with } A_M(\omega_M) = v_M / \omega_M,$$

that is, the movement oscillates (almost) sinusoidally and its amplitude drops hyperbolically with increasing frequency.

3 Discussion

Consistent observations that energy expenditure (oxygen consumption) is lower during episodes of entrainment than nonentrainment (Garlando et al. 1985; Bernasconi and Kohl 1993; Bonsignore et al. 1998) suggest that LRC is a function of aerobic demands. Early investigations of LCR, however, were concerned primarily with identifying its eventual mechanical causes. For instance, Bramble and colleagues formulated an account of LRC in terms of mechanical forces acting on the thorax and diaphragm (Bramble and Carrier 1983), also known as the visceral piston hypothesis. According to this hypothesis, the vertical impulse due to the footfalls induces resonant mechanical vibrations of the diaphragm, thus imposing particular rhythms on the intra-abdominal and thoracic volumes/pressures [see also Bramble and Jenkins (1993)]. Clearly, the thorough investigations of Bramble and colleagues suggest that considerations of the mechanical forces acting on the respiratory system are indispensable for understanding LRC. However, without an explicit account for the efficiency of entrainment, propositions about aerobic demands, mechanics, and coupled oscillators (Amazeen et al. 2001) all remain quite tentative.

In the present study, we showed that LRC might be explained in terms of two self-sustaining oscillators that are coupled via maximization of the (instantaneous) effective value of “energy” (a bilinear form of both oscillatory components) since this coupling readily yields various entrainment patterns as well as transitions between them. The proposed model, which contains only weak nonlinearities, has a fairly rich bifurcation spectrum, similar to the broad range of empirically observed patterns of frequency locking in animals and humans [see, e.g., Boggs (2002) for a recent review]. In the present analyses, we focused specifically on salient dynamic features that were detected in the data of Siegmund et al. (1999), i.e., transitions in frequency locking from 2:1 to 1:1 (1:1 to 1:2) and 90° switches in relative phase. Although our description is qualitative in that we did not consider physiologically motivated oscillator forms and formulated the essential ingredient – the coupling – by means of a simple energy functional, the entrainment patterns do reflect the major empirical findings. Furthermore, and more interestingly, the proposed bifurcation parameters can be interpreted in physiological terms, as will be argued next.

Recall that in our model the movement oscillations describe the intra-abdominal pressure that is known to increase the intrathoracic pressure (Cholewicki et al. 2002). These oscillations may be specified by their amplitudes corresponding to the maximal variation of muscle contraction and by the offset (M_0) around which these oscillations occur. The latter can be interpreted as mean muscle tonus, which apparently affects the frequency ratio in LRC (Fig. 4a). The larger the value M_0 , the more likely it becomes to find a 2:1 entrainment, i.e., a 1:1 frequency locking between stroke rate

and breathing rhythm. Lowering the tonus may induce a transition to a 1:1 coordination pattern, which might subsequently lead to a switch in relative phase within the 1:1 pattern due to changes in movement amplitude. Besides such effects of the movement-related lung pressure, the respiration oscillator may also have differential impacts on the optimal locking mode. For instance, increasing the mean (residual) air volume in the lungs increases the respiration-related pressure and, thus, the value of R_0 . Indeed, this respiration offset may also cause frequency-doubling bifurcations, that is, switches from a 2:1 to a 1:1 entrainment (1:1 to 1:2) (Fig. 4b).

The proposed model combines self-sustaining oscillations in view of a maximization of the resulting energy transfer. The explicit choice of both the oscillators and the energy functional formally reflects (mechanical) constraints on the effective energy. Obviously, the degree to which these constraints are active depends on the specific locomotion adopted and thereby mediates the coupling strength. As a result, depending on the form of locomotion, different (cascades of) frequency locking patterns can be observed. Compared to rowing, many more frequency relations appear to be adopted while running, which might be explained by the rather different frequency regime in which the movement-related lung pressure oscillates. The fast oscillations during running allow for many more integer ratios as all of these are (sub-)optimal and, according to our model, their difference decreases with increasing frequency. Not only do the peak heights of the effective energy at different frequency ratios become similar, their distances become smaller, which could account for the higher incidence of transitions between entrainment patterns during running. Irrespective of the specific activity, however, LRC entrainment always implies a (sub-)optimal energy transfer. Therefore, to be efficient, respiration needs to be frequency locked with cyclic movements at integer ratios. Hence, well-trained individuals reveal LRC more often and more consistently than untrained individuals.

Apart from offering an explanation for frequency locking at ratios composed of small integers, the proposed model here hints at several mechanisms that may cause transitions between entrainment modes, e.g., oscillator offsets, amplitudes, and overall frequency. To date, the number of experimental studies on LRC transitions is rather limited, while those that are available typically fail to pinpoint the precise role of bifurcation parameters. It follows from the present study that, besides movement/respiration tempo and amplitude, mean muscle tonus and mean (residual) air volume in the lungs are also crucial bifurcation parameters to examine in future experiments.

Acknowledgements The contribution of the second author was supported by the Netherlands Organization for Scientific Research (NWO), grant # 425 – 202–01. We would like to thank Gunter Siegmund and David Sanderson for the fruitful discussions and for providing the experimental data that inspired the present study.

References

- Amazeen PG, Amazeen EL, Beek PJ (2001) Coupling of breathing and movement during manual wheelchair propulsion. *J Exp Psychol Hum Percept Perform* 27(5): 1243–1259
- Beek PJ, Rikkert WEI, van Wieringen PCW (1996) Limit cycle properties of rhythmic forearm movements. *J Exp Psychol Hum Percept Perform* 22: 1077–1093
- Bernasconi P, Kohl J (1993) Analysis of co-ordination between breathing and exercise rhythms in man. *J Physiol* 471: 693–706
- Bernasconi P, Burki P, Buhner A, Koller EA, Kohl J (1995) Running training and co-ordination between breathing and running rhythms during aerobic and anaerobic conditions in humans. *Eur J Appl Physiol Occup Physiol* 70(5): 387–393
- Boggs DF (2002) Interactions between locomotion and ventilation in tetrapods. *Comp Biochem Physiol A Mol Integr Physiol* 133(2): 269–288
- Bonsignore MR, Morici G, Abate P, Romano S, Bonsignore G (1998) Ventilation and entrainment of breathing during cycling and running in triathletes. *Med Sci Sports Exerc* 30(2): 239–245
- Bramble DM, Carrier DR (1983) Running and breathing in mammals. *Science* 219(4582): 251–256
- Bramble DM, Jenkins FA Jr (1993) Mammalian locomotor-respiratory integration: implications for diaphragmatic and pulmonary design. *Science* 262(5131): 235–240
- Cholewicki J, Ivancic PC, Radebold A (2002) Can increased intra-abdominal pressure in humans be decoupled from trunk muscle co-contraction during steady state isometric exertions? *Eur J Appl Physiol* 87(2): 127–133
- Del Negro CA, Morgado-Valle C, Feldman JL (2002a) Respiratory rhythm: an emergent network property? *Neuron* 34(5): 821–830
- Del Negro CA, Wilson CG, Butera RJ, Rigatto H, Smith JC (2002b) Periodicity, mixed-mode oscillations, and quasiperiodicity in a rhythm-generating neural network. *Biophys J* 82(1 Pt 1): 206–214
- Garlando F, Kohl J, Koller EA, Pietsch P (1985) Effect of coupling the breathing and cycling rhythms on oxygen uptake during bicycle ergometry. *Eur J Appl Physiol Occup Physiol* 54(5): 497–501
- Glass L (2001) Synchronization and rhythmic processes in physiology. *Nature* 410(6825): 277–284
- Guckenheimer J, Holmes P (1983) Nonlinear oscillations, dynamical systems, and bifurcations of vector fields. Springer, Berlin Heidelberg New York
- Haken H (1996) Principles of brain functioning. Springer, Berlin Heidelberg New York
- Haken H (2000) Information and self-organization: a macroscopic approach to complex systems. Springer, Berlin Heidelberg New York
- Hoppensteadt FC (1997) An introduction to the mathematics of neurons: modeling in the frequency domain. Cambridge University Press, Cambridge, UK
- Kay BAK, Kelso JAS, Saltzman E, Schöner G (1987) Space-time behavior of single and bimanual rhythmic movements. *J Exp Psychol Hum Percept Perf* 13: 178–192
- Keith WL, Rand RH (1984) 1:1 and 2:1 phase entrainment in a system of two limit cycle oscillators. *J Math Biol* 20: 133–152
- Kelso JAS (1995) Dynamic patterns: the self-organization of brain and behavior. MIT Press, Cambridge, MA
- Kohl J, Koller EA, Jager M (1981) Relation between pedalling and breathing rhythm. *Eur J Appl Physiol Occup Physiol* 47(3): 223–237
- Mahler DA, Hunter B, Lentine T, Ward J (1991a) Locomotor-respiratory coupling develops in novice female rowers with training. *Med Sci Sports Exerc* 23(12): 1362–1366
- Mahler DA, Shuhart CR, Brew E, Stukel TA (1991b) Ventilatory responses and entrainment of breathing during rowing. *Med Sci Sports Exerc* 23(2): 186–192
- Manning TS, Plowman SA, Drake G, Looney MA, Ball TE (2000) Intra-abdominal pressure and rowing: the effects of inspiring versus expiring during the drive. *J Sports Med Phys Fitness* 40(3): 223–232
- Nayfeh AH, Mook DT (1979) Nonlinear oscillations. Wiley, New York
- Nicolis G, Prigogine I (1989) Exploring complexity: an introduction. Freeman, New York
- Rodriguez RJ, Rogriguez RP, Cook SD, Sandborn PM (1990) Electromyographic analysis of rowing stroke biomechanics. *J Sports Med Phys Fitness* 30(1): 103–108
- Siegmund GP, Edwards MR, Moore KS, Tiessen DA, Sanderson DJ, McKenzie DC (1999) Ventilation and locomotion coupling in varsity male rowers. *J Appl Physiol* 87(1): 233–242
- Wasjwelner H, Bennell K, Story I, McKeenan J (2000) Muscle action and stress on the ribs in rowing. *Phys Ther Sport* 1: 75–84
- Young IS, Warren RD, Altringham JD (1992) Some properties of the mammalian locomotory and respiratory systems in relation to body mass. *J Exp Biol* 164: 283–294